Chapter 13

Thermal Properties

What happens in these Lattices when Heat
Transports Vibrations through a solid mass?
T = 3Nk is much too neat;
A rigid Crystal's not a fluid Gas.
Debye *in 1912 proposed Elas-*
Tic Waves called phonons that obey Max Planck's
E = hν. Though amorphous Glass,
Umklapp *Switchbacks, and Isotopes play pranks*
Upon his Formulae, Debye *deserves warm Thanks.*

John Updike, *The Dance of the Solids*[†]

13.1 Introduction

As a consequence of their brittleness and their low thermal conductivities, ceramics are prone to thermal shock; i.e., they will crack when subjected to large thermal gradients. This is why it is usually not advisable to pour a very hot liquid into a cold glass container, or cold water on a hot ceramic furnace tube — the rapidly cooled surface will want to contract, but will be restrained from doing so by the bulk of the body, so stresses will develop. If these stresses are large enough, the ceramic will crack.

Thermal stresses will also develop because of thermal contraction mismatches in multiphase materials or anisotropy in a single phase. It thus follows that thermal stresses exist in all polycrystalline ceramics with noncubic structures that undergo phase transformations or include second phases with differing thermal expansion characteristics. These stresses can result in the formation of stable microcracks and can strongly influence the strength and fracture toughness of ceramics. In a worst-case scenario, these stresses can cause the total disintegration of a ceramic body. Used properly, however, they can enhance the strength of glasses. The purpose of this chapter is to

[†] J. Updike, *Midpoint and other Poems*, A. Knopf, Inc., New York, New York, 1969. Reprinted with permission.

explore the problem of thermal residual stresses, why they develop and how to quantify them.

Another important thermal property dealt with in Sec. 13.6 is thermal conductivity. It is the low thermal conductivity of ceramics, together with their chemical inertness and oxidation resistance, that renders them as a class of materials uniquely qualified to play an extremely demanding and critical role during metal smelting and refining. Many ceramics such as diaspore, alumina, fosterite, and periclase are used for the fabrication of high-temperature insulative firebrick without which the refining of some metals would be impossible.

13.2 Thermal Stresses

The Origin of Thermal Residual Stresses

As noted above, thermal stresses can be induced by differential thermal expansion in multiphase materials or anisotropy in the thermal expansion coefficients of single-phase solids. The latter is treated in Sec. 13.4. To best illustrate the idea of how differential thermal expansion in multiphase materials leads to thermal stresses, consider the simple case shown schematically in Fig. 13.1*a*, where a solid disk is placed inside of a ring of a different

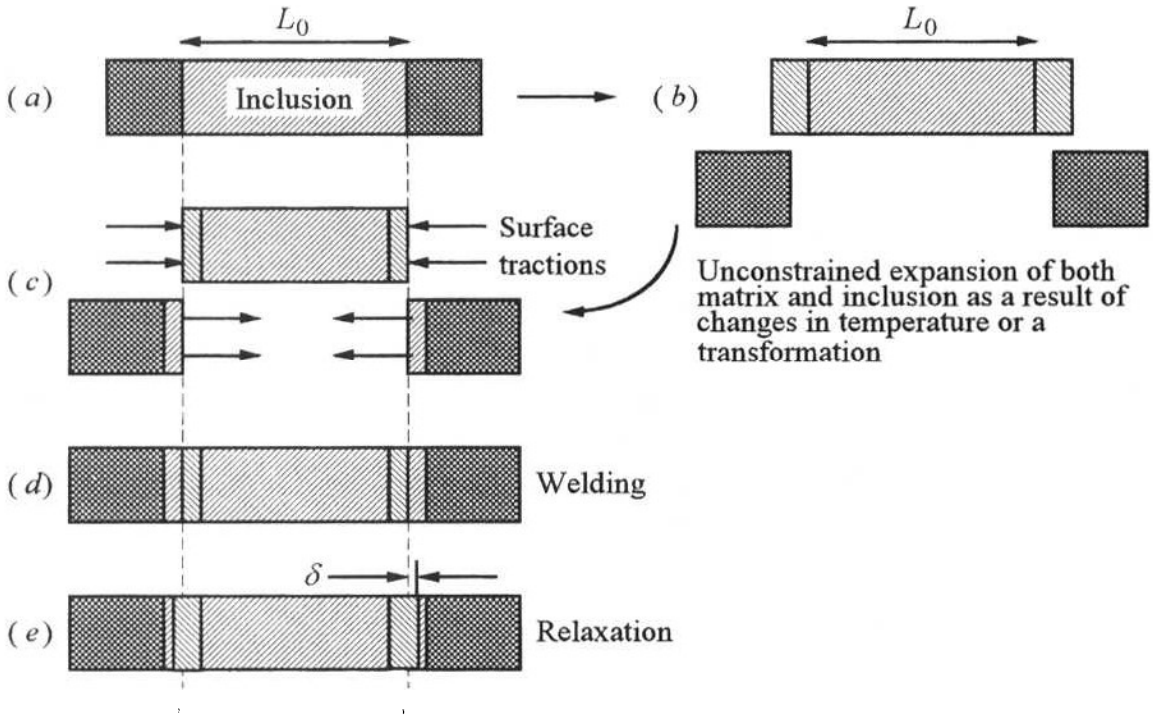

Figure 13.1 Steps involved in Eshellby's method. (*a*) Initial configuration. (*b*) Cutting and allowing for free expansion of both inclusion and matrix as a result of heating. Note that the radius of the outside ring increases upon heating. (*c*) Application of surface forces needed to restore elements to original shape. (*d*) Weld pieces together. (*e*) Allow the system to relax. Note displacement of original interface as a result of relaxation.

material. To emphasize the similarity of this problem to that of an inclusion in a matrix, which was discussed in Chap. 11 and is one of practical significance, the disk will henceforth be referred to as the *inclusion*, and the outside ring as the *matrix*, with thermal expansion coefficients α_i and α_m, respectively.

Before one attempts to find a quantitative answer, it is important to qualitatively understand what happens to such a system as the temperature is varied. Needless to say, the answer will depend on the relative values of α_i and α_m, and whether the system is being heated or cooled. To illustrate, consider the case where $\alpha_i > \alpha_m$ and the system is heated. Both the inclusion and the matrix will expand[231] (Fig. 13.1*b*); however, given that $\alpha_i > \alpha_m$, the inclusion will try to expand at a faster rate, but will be radially restricted from doing so by the outside ring. It follows that upon heating, both the inclusion and the matrix will be in radial compression. It is left as an exercise to the reader to show that if the assembly were cooled, the inclusion would develop radial tensile stresses. It should be noted here, and is discussed in greater detail below, that stresses other than radial also develop.

The quantification of the problem is nontrivial and is usually carried out today by using finite-element and other numerical techniques. However, for simple geometries, a powerful method developed by Eshellby[232] exists, which in principle is quite simple, elegant, and ingenious. The problem is solved by carrying out the following series of imaginary cuts, strains, and welding operations illustrated in Fig. 13.1:

1. Cut the inclusion out of the matrix.
2. Allow both the inclusion and the matrix to expand or contract as a result of either heating or cooling (or as a result of a phase transformation) (Fig. 13.1*b*).
3. Apply sufficient surface traction to restore the elements to their original shape (Fig. 13.1*c*).
4. Weld the pieces together (Fig. 13.1*d*).
5. Allow the system to relax (Fig. 13.1*e*).

To apply this technique to the problem at hand, do the following:

1. Cut the inclusion, and allow both it and the matrix to freely expand (Fig. 13.1*b*). The thermal strain in the inclusion is given by [Eq. (4.2)]:

$$\frac{\Delta L}{L_0} = \varepsilon_i = \alpha_i \Delta T = \alpha_i (T_{\text{final}} - T_{\text{init}})$$

$$\boxed{\varepsilon_i = \alpha_i (T_{\text{final}} - T_{\text{init}})} \tag{13.1}$$

[231] Note that the expansion of the matrix implies that the internal diameter of the ring increases with increasing temperature.

[232] J. D. Eshellby, *Proc. Roy. Soc.*, **A241**:376–396 (1957).

Similarly, for the matrix

$$\varepsilon_m = \alpha_m \Delta T \tag{13.2}$$

Note that as defined here, ΔT *is positive during heating and negative during cooling*. On cooling, T_{final} is usually taken to be room temperature; T_{init}, however, is more difficult to determine unambiguously, but it *is the highest temperature below which the residual stresses are not relieved*, which, depending on the material in question, may or may not be identical to the processing or annealing temperature. At high enough temperatures, stress relaxation by diffusive or viscous flow will usually relieve some, if not most, of the residual stresses; it is only below a certain temperature that these stress relaxation mechanisms become inoperative and local elastic residual stresses start to develop from the contraction mismatch.

2. Apply a stress to each element to restore it to its original shape[233] (Fig. 13.1*c*). For the inclusion,

$$\sigma_i = -Y_i \varepsilon_i = -Y_i \alpha_i \Delta T \tag{13.3}$$

where Y is Young's modulus. For the matrix:

$$\sigma_m = Y_m \varepsilon_m = Y_m \alpha_m \Delta T \tag{13.4}$$

Note that the applied stress needed to restore the inclusion to its original shape is compressive (see Fig. 13.1*c*), which accounts for the minus sign in Eq. (13.3).

3. Weld the two parts back together (Fig. 13.1*d*), and allow the stresses to relax. Since the stresses are unequal, one material will "push" into the other, and the location of the *original interface will shift by a strain* δ in the direction of the larger stress until the two stresses are equal (Fig. 13.1*e*). At equilibrium the two radial stresses are equal and are given by

$$\sigma_{i,\text{eq}} = Y_i[\varepsilon_i + \delta] = \sigma_{m,\text{eq}} = Y_m[\varepsilon_m - \delta] \tag{13.5}$$

Solving for δ, plugging that back into Eq. (13.5), and making use of Eqs. (13.1) to (13.4), one can show (see Prob. 13.2) that

$$\sigma_{i,\text{eq}} = \sigma_{m,\text{eq}} = \frac{\Delta\alpha \Delta T}{1/Y_i + 1/Y_m} = \frac{(\alpha_m - \alpha_i)\Delta T}{1/Y_i + 1/Y_m} \tag{13.6}$$

This is an important result which predicts that

- If $\Delta\alpha$ is zero, no stress develops, which makes sense since the matrix and the inclusion would be expanding at the same rate.
- For $\alpha_i > \alpha_m$, upon heating (positive ΔT), the stresses generated in the inclusion and matrix should be compressive or negative, as anticipated.

[233] Equations (13.2) and (13.3) are strictly true only for a one-dimensional problem. Including the other dimensions does not generally greatly affect the final result [see Eq. (13.8)].

- If the inclusion is totally *constrained from moving* (that is, $\alpha_m = 0$ and Y_m is infinite), then Eq. (13.6) simplifies to the more familiar equation

$$\sigma_{i,\text{eq}} = -Y_i \alpha_i \Delta T \tag{13.7}$$

which predicts that upon heating, the stress generated will be compressive, and vice versa upon cooling.

In treating the system shown in Fig. 13.1, for simplicity's sake, only the radial stresses were considered. The situation in three dimensions is more complicated, and it is important at this stage to be able to at least qualitatively predict the nature of these stresses. Since the problem is no longer one-dimensional, in addition to the radial stresses, the **axial** and **tangential** or **hoop stresses** have to be considered.

To qualitatively predict the nature of these various stresses, a useful trick is to assume the lower thermal expansion coefficient of the two components to be zero and to carry out the Eshellby technique. To illustrate, consider the nature of the thermal residual stresses that would be generated if a fiber with expansion coefficient α_f were embedded in a matrix (same problem as the one shown in Fig. 13.1, except that now the three-dimensional state of stress is of interest), densified, and *cooled* from the processing temperature for the case when $\alpha_m > \alpha_f$. Given that $\alpha_m > \alpha_f$ and by making use of the aforementioned trick, i.e., by assuming $\alpha_f = 0$ (which implies its dimension does not change with temperature changes), it follows that upon cooling, the matrix will shrink both axially and radially (the hole will get smaller). Consequently, the stress required to fit the matrix to the fiber will have to be axially tensile; when the matrix is welded to the fiber and allowed to relax, this will place the fiber in a state of axial residual compressive stress, which, in turn, is balanced by an axial tensile stress in the matrix. Radially, the matrix will clamp down on the fiber, resulting in radial compressive stresses in both the fiber and the matrix, in agreement with the conclusions drawn above. In addition, the system will develop tensile tangential stresses, as shown in Fig. 13.2*a*.[234] These stresses, if sufficiently high, can cause the matrix to crack radially as shown in Fig. 13.2*c*. It is left as an exercise to readers to determine the state of stress when $\alpha_m < \alpha_f$, and to compare their results with those summarized in Fig. 13.2*b*.

Finally, in this section the problem of a spherical inclusion in an infinite matrix is considered. It can be shown that the radial (σ_{rad}) and tangential (σ_{tan}) stresses generated for a spherical inclusion of radius R at a distance

[234] To appreciate the nature of tangential stresses, it helps to go back to the Eshellby technique and ask, What would be required to make the hole in the matrix, which is now smaller than the fiber it surrounds, larger? The answer is, One would have to stretch the matrix in a manner similar to fitting a smaller-diameter hose around a larger-diameter pipe. This naturally results in a tangential stress in the hose. Experience tells us that if the hose is too small, it will develop radial cracks similar to the one shown in Fig. 13.2*c*.

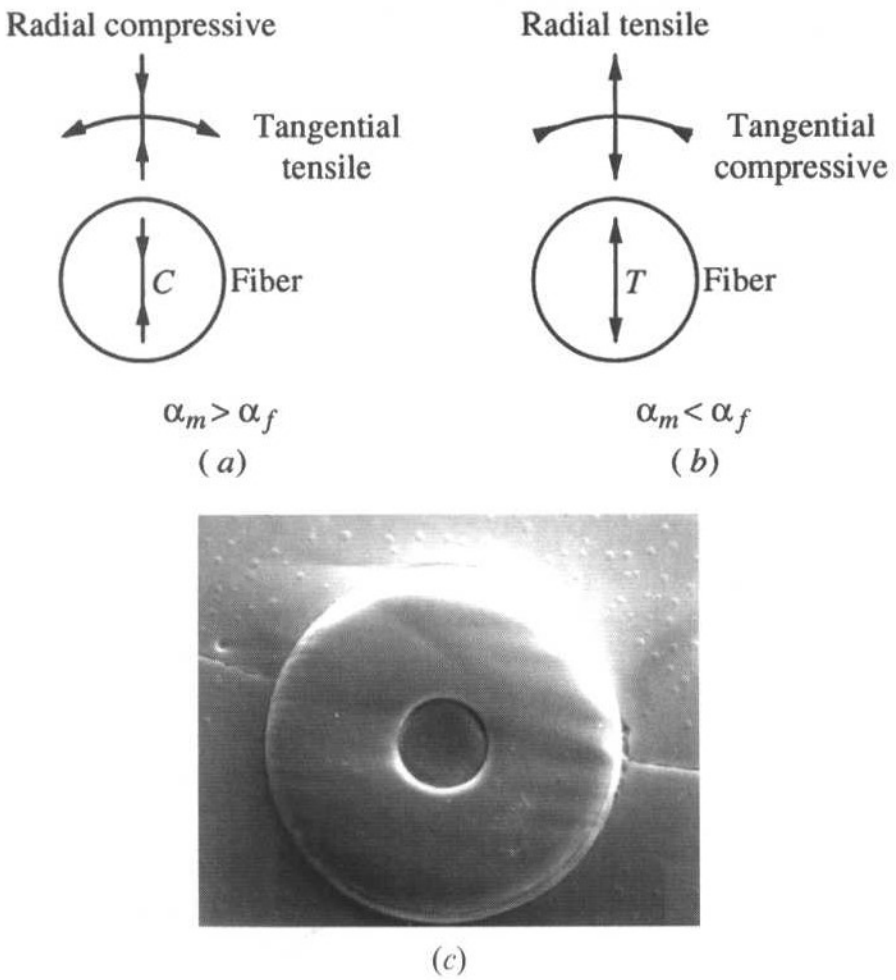

Figure 13.2 Radial and tangential stresses developed upon cooling of a fiber embedded in a matrix for (*a*) $\alpha_m < \alpha_f$ and (*b*) $\alpha_m > \alpha_f$. (*c*) Micrograph of radial cracks generated around a fiber upon cooling when $\alpha_m > \alpha_f$.

r away from the interface are given by:

$$\sigma_{\text{rad}} = -2\sigma_{\text{tan}} = \frac{(\alpha_m - \alpha_i)\Delta T}{(1 - 2\nu_i)/Y_i + (1 + \nu_m)/(2Y_m)} \left(\frac{R}{r + R}\right)^3 \tag{13.8}$$

where ν_i and ν_m are, respectively, Poisson's ratio for the inclusion and matrix. The stress is a maximum at the interface, i.e., at $r = 0$, and drops rapidly with distance. Note that the final form of this expression is similar to Eq. (13.6). It is worth noting here that the Eshellby technique is not restricted to calculating thermal stresses; also, it can be used to calculate transformation stresses.

13.3 Thermal Shock

Generally speaking, thermal stresses are to be avoided since they can significantly weaken a component. In extreme cases, a part can spontaneously crumble during cooling. As noted earlier, *rapid* heating or cooling of a

ceramic will often result in its failure. This kind of failure is known as *thermal shock* and occurs when thermal gradients and corresponding thermal stresses exceed the strength of the part. For instance, as a component is rapidly cooled from a temperature T to T_0, the surface will tend to contract but will be prevented from doing so by the bulk of the component that is still at temperature T. By using arguments similar to the ones made above, it is easy to appreciate that in such a situation surface tensile stresses would be generated that have to be counterbalanced by compressive ones in the bulk.

Experimental Details: Measuring Thermal Shock Resistance

Thermal shock resistance is usually evaluated by heating samples to various temperatures T_{max}. The samples are rapidly cooled by quenching them from T_{max} into a medium, most commonly ambient temperature water. The post-quench retained strengths are measured and plotted versus the severity of the quench, or $\Delta T = T_{max} - T_{ambi}$. Typical results of such experiments are shown in Fig. 13.3*a*, where the salient feature is the occurrence of a rapid decrease in retained strength around a critical temperature difference ΔT_c below which the original strength is retained. As the quench temperature is further increased, the strength decreases but more gradually. Actual data for single-crystal and polycrystalline alumina are shown in Fig. 13.3*b*.

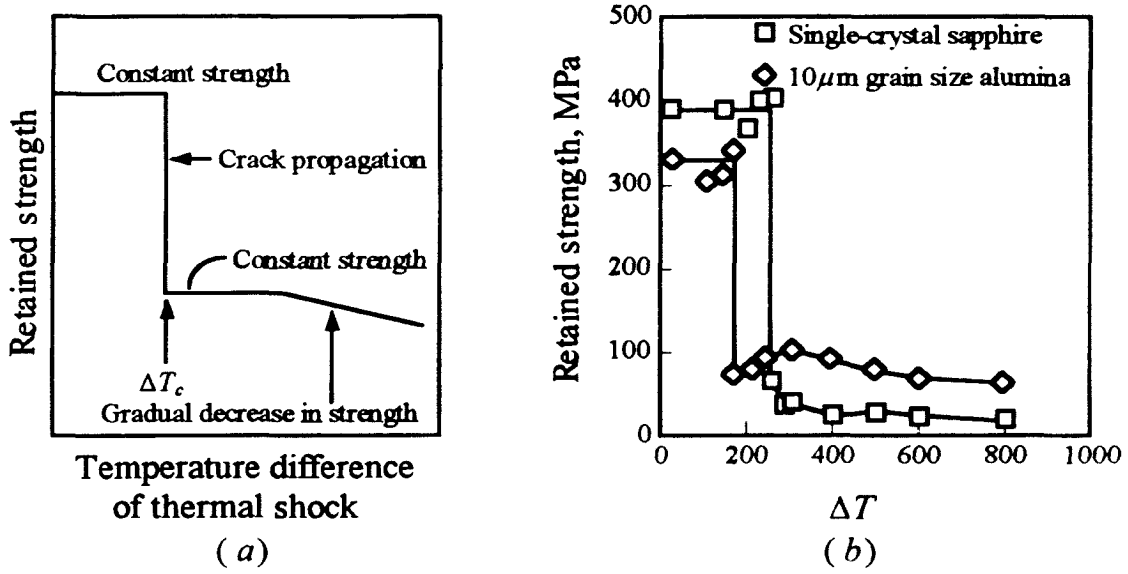

Figure 13.3 (*a*) Schematic of strength behavior as a function of severity of quench ΔT. (*b*) Actual data for single-crystal and polycrystalline alumina[235] (error bars were omitted for the sake of clarity).

[235] T. K. Gupta, *J. Amer. Cer. Soc.*, **55**:249 (1972).

From a practical point of view, it is important to be able to predict ΔT_c. Furthermore, it is only by understanding the various parameters that affect thermal shock that successful design of solids which are resistant to it can be carried out. In the remainder of this section, a methodology is outlined for doing just that, an exercise that will by necessity highlight the important parameters that render a ceramic resistant to thermal shock.

To estimate ΔT_c, the following assumptions are made[236]

1. The material contains N identical, uniformly distributed, Griffith flaws per unit volume.
2. The flaws are circular with radii c_i.
3. The body is uniformly cooled with the external surfaces rigidly constrained to give a well-defined triaxial tensile state of stress given by[237]

$$\sigma_{\text{ther}} = -\frac{\alpha Y \Delta T}{(1-2\nu)} \tag{13.9}$$

4. Crack propagation occurs by the simultaneous propagation of the N cracks, with negligible interactions between the stress fields of neighboring cracks.

The derivation is straightforward and follows the one carried out in deriving Eq. (11.9). The total energy of the system can be expressed as

$$U_{\text{tot}} = U_0 - U_{\text{strain}} + U_{\text{surf}}$$

where U_0 is the energy of the stress- and crack-free crystal of volume V_0; U_{surf} and U_{strain} are, respectively, the surface and strain energies of the system. Since it was assumed that the stress fields were noninteracting, in the presence of N cracks U_{tot} is modified to read

$$U_{\text{tot}} = U_0 + \frac{V_0 \sigma_{\text{ther}}^2}{2Y} - \frac{N\sigma_{\text{ther}}^2}{2Y}\frac{4\pi c_i^3}{3} + NG_c \pi c_i^2 \tag{13.10}$$

where the third term on the right-hand side represents the strain energy released by the existence of the cracks and the last term is the energy needed to extend them. G_c is toughness of the material (Eq. (11.11)).

Differentiating this expression with respect to c_i, equating the resulting expression to zero, and rearranging terms, one can easily show (see Prob. 13.6*a*) that for $\Delta T > \Delta T_c$, where ΔT_c is given by

$$\Delta T_c \geq \sqrt{\frac{G_c(1-2\nu)^2}{\alpha^2 Y c_i}} \tag{13.11}$$

the cracks will grow and release the strain energy. Conversely, for $\Delta T \leq \Delta T_c$, the strain energy that develops is insufficient to extend the

[236] The derivation shown here is a simplified version of one originally outlined by D. P. H. Hasselman, *J. Amer. Cer. Soc.*, **46**:453 (1963) and **52**:600 (1969).

[237] Note similarity of this equation to Eq. (13.7).

cracks, which in turn implies that the strength should remain unchanged, as experimentally observed.

In contrast to the situation of a flaw propagating as a result of a constant applied stress, in which the flaw will extend indefinitely until fracture, the driving force for crack propagation during thermal shock is finite. In the latter case, the cracks will only extend up to a certain length c_f that is commensurate with the strain energy available to them and then stop. To estimate c_f, one simply equates the strain energy available to the system to the increase in surface energy, or

$$\pi N G_c (c_f^2 - c_i^2) = \frac{(\alpha \Delta T_c)^2 Y}{2(1-2\nu)^2} \tag{13.12}$$

For short initial cracks, that is, $c_f \gg c_i$, substituting for the value of ΔT_c from Eq. (13.11), one obtains

$$c_f \cong \sqrt{\frac{1}{\pi N c_i}} \tag{13.13}$$

which interestingly enough does not depend on any material parameters.

For the sake of clarity, the model used to derive Eqs. (13.11) and (13.13) was somewhat simplified. Using a slightly more sophisticated approach, Hasselman obtained the following relationships:

$$\boxed{\Delta T_c = \sqrt{\frac{\pi G_c (1-2\nu)^2}{Y \alpha^2 (1-\nu^2) c_i} \left[1 + \frac{16 N c_i^3 (1-\nu)^2}{9(1-2\nu)}\right]}} \tag{13.14}$$

$$c_f = \sqrt{\frac{3(1-2\nu)}{8(1-\nu^2) N c_i}} \tag{13.15}$$

And while at first glance these expressions may appear different from those derived above, on closer examination, their similarity becomes obvious. For example, for small cracks of low density, the second term in brackets in Eq. (13.14) can be neglected with respect to unity, in which case, but for a few terms including Poisson's ratio and π, Eq. (13.14) is similar to Eq. (13.11). The same is true for Eqs. (13.13) and (13.15).

Before one proceeds further, it is worthwhile to summarize the physics of events occurring during thermal shock. Subjecting a solid to a rapid change in temperature results in differential dimensional changes in various parts of the body and a buildup of stresses within it. Consequently, the strain energy of the system will increase. If that strain energy increase is not too large, i.e., for small ΔT values, the preexisting cracks will not grow and the solid will not be affected by the thermal shock. However, if the thermal shock is large, the many cracks present in the solid will extend and absorb the excess strain energy. Since the available strain energy is finite, the

cracks will extend only until most of the strain energy is converted to surface energy, at which point they will be arrested. The final length to which the cracks will grow will depend on their initial size and density. If only a few, small cracks are present, their final length will be large and the degradation in strength will be high. Conversely, if there are numerous small cracks, each will extend by a small amount and the corresponding degradation in strength will not be that severe. In the latter case, the solid is considered to be **thermal-shock-tolerant**.

It is this latter approach that is used in fabricating insulating firebricks for furnaces and kilns. The bricks are fabricated so as to be porous and contain many flaws. Because of the very large number of flaws and pores within them, the bricks can withstand severe thermal cycles without structural failure.

Inspecting Eq. (13.11) or (13.14), it is not difficult to conclude that a good figure of merit for thermal shock resistance is

$$\boxed{R_H = (\text{const})(\Delta T_c) = (\text{const})\sqrt{\frac{G_c}{\alpha^2 Y}} = \frac{K_{Ic}}{\alpha Y}} \tag{13.16}$$

from which it is clear that ceramics with low thermal expansion coefficients, low elastic moduli, but high fracture toughnesses should be resistant to thermal shock.

Kingery's[238] approach to the problem was slightly different. He postulated that failure would occur when the thermal stress, given by Eq. (13.7), was equal to the tensile strength σ_t of the specimen (see Prob. 13.4). By equating the two, it can be shown that the figure of merit in this case is

$$R_{TS} = (\text{const})(\Delta T_c) = (\text{const})\frac{(1-2\nu)\sigma_t}{\alpha Y} \tag{13.17}$$

However, given that σ_t is proportional to $(G_c Y/c_{\max})^{1/2}$, it is an easy exercise to show that R_{TS} is proportional to $R_H/c_{\max}^{1/2}$, implying that the two criteria are related.[239]

One parameter which is not included in either model, and which clearly must have an important effect on thermal shock resistance, is the thermal conductivity of the ceramic k_{th} (see Sec. 13.6). Given that thermal gradients are ultimately responsible for the buildup of stress, it stands to reason that a highly thermally conductive material would not develop large gradients and would thus be thermal shock resistant. For the same reason, the heat capacity and the heat-transfer coefficient between the solid and the environment must also play a role. Thus an even better indicator of thermal shock

[238] W. D. Kingery, *J. Amer. Cer. Soc.*, **38**:3–15 (1955).

[239] It is interesting to note that the Hasselman solid is a highly idealized one where all the flaws are the same size.

Table 13.1 Comparison of thermal shock parameters for a number of ceramics. Poisson's ratio was taken to be 0.25 for all materials

Material	MOR, MPa	Y, GPa	α, $10^6\,K^{-1}$	k_{th}, W/(m·K)	K_{Ic}, MPa·m$^{1/2}$	$k_{th}R_{TS}$, W/m	$R_H k_{th}$, W/m^2	ΔT_c, exper.
SiAlON	945	300	3.0	21	7.7	16,500	180	900
HP†–Si_3N_4	890	310	3.2	15–25	5.0	16,800	126	500–700
RB‡–Si_3N_4	240	220	3.2	8–12	2.0	2,557	28	≈500
SiC (sintered)	483	410	4.3	84	3.0	17,300	143	300–400
HP†–Al_2O_3	380	400	9.0	6–8	3.9	633	8	200
HP†–BeO	200	400	8.5	63		2,800		
PSZ	610	200	10.6	2	≈10.0	435	9	500
Ti_3SiC_2	300	320	9.1	43	≈10.0		149	>1400

† Hot-pressed

‡ Reaction-bonded

§ Partially stabilized zirconia

resistance is to multiply Eq. (13.16) or (13.17) by k_{th}. These values are calculated for a number of ceramics and listed in Table 13.1 in columns 7 and 8. Also listed in Table 13.1 are the experimentally determined values. A correlation between the two sets of values is apparent, giving validity to the aforementioned models.

Note that in general the nitrides and carbides of Si, with their lower thermal expansion coefficients, are more resistant to thermal shock than oxides. In theory, a material with zero thermal expansion would not be susceptible to thermal shock. In practice, a number of such materials do actually exist commercially, including some glass-ceramics that have been developed which, as a result of thermal expansion anisotropy, have extremely low α's (see Ch. 4). Another good example is fused silica which also has an extremely low α and thus is not prone to thermal shock.

13.4 Spontaneous Microcracking of Ceramics

In the previous section, the emphasis was on thermal shock, where failure was initiated by a *rapid and/or severe temperature change*. This is not always the case; both single- and multiphase ceramics have been known to spontaneously microcrack upon cooling. Whereas thermal shock can be avoided by slow cooling, the latter phenomenon is *unavoidable* regardless of the rate at which the temperature is changed.

Spontaneous microcracking results from the buildup of residual stresses which can be caused by one or more of the following three reasons:

- Thermal expansion anisotropy in single-phase materials

Table 13.2 Thermal expansion coefficients for some ceramic crystals with anisotropic thermal expansion behavior

Material	Normal to c axis	Parallel to c axis
Al_2O_3	8.3	9.0
Al_2TiO_5	−2.6	11.5
$3Al_2O_3 \cdot 2SiO_2$ (mullite)	4.5	5.7
$CaCO_3$	−6.0	25.0
$LiAlSi_2O_6$ (β-spodumene)	6.5	−2.0
$LiAlSiO_4$ (β-eucryptite)	8.2	−17.6
$NaAlSi_3O_8$ (albite)	4.0	13.0
SiO_2 (quartz)	14.0	9.0
TiO_2	6.8	8.3
$ZrSiO_4$	3.7	6.2

- Thermal expansion mismatches in multiphase materials
- Phase transformations and accompanying volume changes in single- or multiphase materials

In the remainder of this section each of these cases is explored in some detail.

13.4.1 Spontaneous Microcracking due to Thermal Expansion Anisotropy

Noncubic ceramics with high thermal expansion anisotropy have been known to spontaneously microcrack upon cooling.[240] The cracking, which occurs along the grain boundaries, becomes progressively less severe with decreasing grain size, and below a certain "critical" grain size, it is no longer observed. The phenomenon has been reported for various solids such as Al_2O_3, graphite, Nb_2O_5, and many titania-containing ceramics such as TiO_2, Al_2TiO_5, Mg_2TiO_5, and Fe_2TiO_5. Data for some anisotropic crystals are given in Table 13.2.

Before one attempts to quantify the problem, it is important once again to understand the underlying physics. Consider the situation shown in Fig. 13.4*a*, where the grains, assumed to be cubes, are arranged in such a way that adjacent *grains* have different thermal expansion coefficients along their x and y axes as shown, with $\alpha_1 < \alpha_2$. To further elucidate the problem, use the aforementioned trick of equating the lower thermal expansion to zero, i.e. pretend $\alpha_1 = 0$. If during cooling the grains are unconstrained, the shape of the assemblage would be that shown in Fig. 13.4*b*. But the cooling is *not* unconstrained, which implies that a buildup of stresses

[240] The thermal expansion coefficients of cubic materials are isotropic and hence do not exhibit this phenomenon.

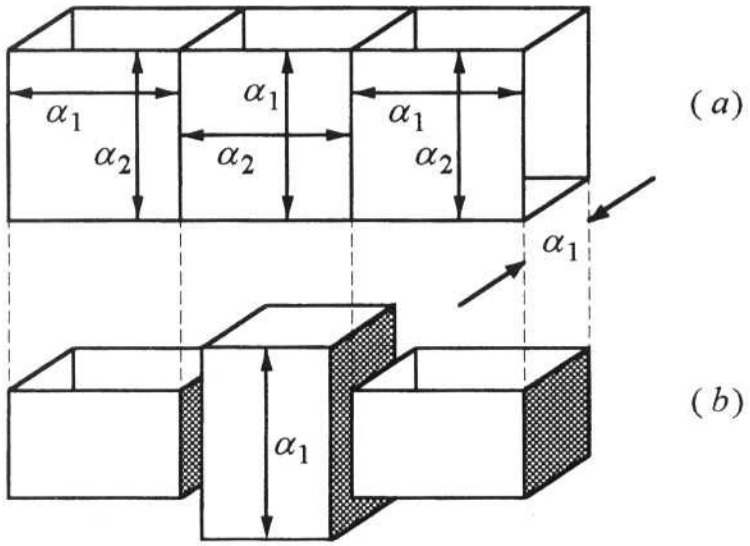

Figure 13.4 Schematic of how thermal expansion anisotropy can lead to the development of thermal stresses upon cooling of a polycrystalline solid. (*a*) Arrangement of grains prior to cooling shows relationship between thermal expansion coefficients and grain axis. (*b*) Unconstrained contraction of grains. Here it was assumed that $\alpha_1 = 0$.

at the boundaries will occur. It is this stress that is ultimately responsible for failure.

To estimate the critical grain size above which spontaneous microcracking would occur, the various energy terms have to be considered. For the sake of simplicity, the grains are assumed to be cubes with grain size d in which case the total energy of the system is[241]

$$U_{\text{tot}} = U_s - NU_g d^3 + 6Nd^2 G_{c.\text{gb}} \tag{13.18}$$

where N is the number of grains relieving their stress and $G_{c.\text{gb}}$ is the grain boundary toughness; U_s is the energy of the unmicrocracked body, and U_g is the strain energy per unit volume stored in the grains. Differentiating Eq. (13.18) with respect to d and equating to zero yields the critical grain size

$$d_{\text{crit}} = \frac{4G_{c.\text{gb}}}{U_g} \tag{13.19}$$

U_g is estimated as follows: For a totally constrained grain, the stress developed is given by Eq. (13.7). Extending the argument to two adjacent grains, the residual stress can be approximated by

$$\sigma_{\text{th}} = \tfrac{1}{2} Y \Delta\alpha_{\max} \Delta T \tag{13.20}$$

where $\Delta\alpha_{\max}$ is the maximum anisotropy in thermal expansion between two crystallographic directions. Substituting Eq. (13.20) in the expression for the

[241] The treatment here is a slightly simplified version of that carried out by J. J. Cleveland and R. C. Bradt, *J. Amer. Cer.*, **61**:478 (1978).

strain energy per unit volume, that is, $U_g = \sigma^2/(2Y)$, and combining with Eq. (13.19), one obtains

$$d_{\text{crit}} = \frac{32G_{c,\text{gb}}}{Y\Delta\alpha_{\max}^2\Delta T^2} \tag{13.21}$$

In general, however,

$$\boxed{d_{\text{crit}} = (\text{const})\frac{G_{c,\text{gb}}}{Y\Delta\alpha_{\max}^2\Delta T^2}} \tag{13.22}$$

where the value of the numerical constant one obtains depends on the details of the models. This model predicts that the critical grain size below which spontaneous microcracking will *not* occur is a function of the thermal expansion anisotropy, the grain boundary fracture toughness, and Young's modulus. Experimentally, the functional relationship among d_{crit}, ΔT, and $\Delta\alpha_{\max}$ is reasonably well established (see Prob. 13.8).

Experimental Details: Determination of Microcracking

Unless a ceramic component totally falls apart in the furnace as the sample is cooled from the sintering or processing temperature, it is experimentally difficult to observe directly grain boundary microcracks. There are, however, a number of indirect techniques to study the phenomenon. One is to fabricate ceramics of varying grain sizes and measure their flexural strengths after cooling. A dramatic decrease in strength over a narrow grain size variation is usually a good indication that spontaneous microcracking has occurred.

13.4.2 Spontaneous Microcracking due to Thermal Expansion Mismatches in Multiphase Materials

Conceptually there is little difference between this situation and the preceding one; the similarity of the two cases is easily appreciated by simply replacing one of the grains in Fig. 13.4 by a second phase with a different thermal expansion coefficient from its surroundings.

13.4.3 Spontaneous Microcracking due to Phase-Transformation-Induced Residual Stresses

Here the residual stresses do not develop as a result of thermal expansion mismatches or rapid variations in temperature, but as a result of phase transformations. Given that these transformations entail atomic rearrangements, they are always associated with a volume changes (e.g., Fig. 4.5). Conceptually, the reason why such a volume change should give rise to residual

stresses should at this point be obvious. Instead of using $\Delta\alpha$, however, the resultant stresses usually scale with $\Delta V/V_0$, where ΔV is the volume change associated with the transformation. The stresses approximated by

$$\sigma \approx \frac{Y}{3(1-2\nu)} \frac{\Delta V}{V_0} \tag{13.23}$$

can be quite large. For example, a 3 percent volumetric change in a material having a Y of 200 GPa and Poisson's ratio of 0.25 would provide a stress of about 4 GPa!

Residual stresses are generally deleterious to the mechanical properties and should be avoided. This is especially true if a part is to be subjected to thermal cycling. In some situations, however, residual stresses can be used to advantage. A case in point is the transformation toughening of zirconia discussed in Chap. 11, and another excellent example is the tempering of glass discussed in the next section.

13.5 Thermal Tempering of Glass

Because of the transparency and chemical inertness of inorganic glasses, their uses in everyday life are ubiquitous. However, for many applications, especially where safety is concerned, as manufactured, glass is deemed to be too weak and brittle. Fortunately, glass can be significantly strengthened by a process referred to as *thermal tempering*, which introduces a state of compressive residual stresses on the surface (see Sec. 11.3.3).

The appropriate thermal process, illustrated in Fig. 13.5, involves heating the glass body to a temperature above its glass transition temperature, followed by a two-step quenching process. During the first quenching stage, initially the surface layer contracts more rapidly than the interior and becomes rigid while the interior is still in a viscous state. This results in a tensile state of stress at the surface, shown in Fig. 13.5*c*. However, since the interior is viscous these stresses will relax, as shown in Fig. 13.5*d*.

During the second quenching step, the entire glass sample is cooled to room temperature. Given that on average the glass interior will have cooled at a *slower* rate than its exterior, its final specific volume will be *smaller* than that of the exterior.[242] The situation is shown in Fig. 13.5*e* and leads directly to the desired final state of stress (Fig. 13.5*f*) in which the external surfaces are in compression and the interior is in tension.

[242] This effect was discussed briefly in Sec. 9.4.1 and illustrated in Fig. 9.8*a*. Simply put, the more time the atoms have to arrange themselves during the cooling process (slow cooling rate), the denser the glass that results.

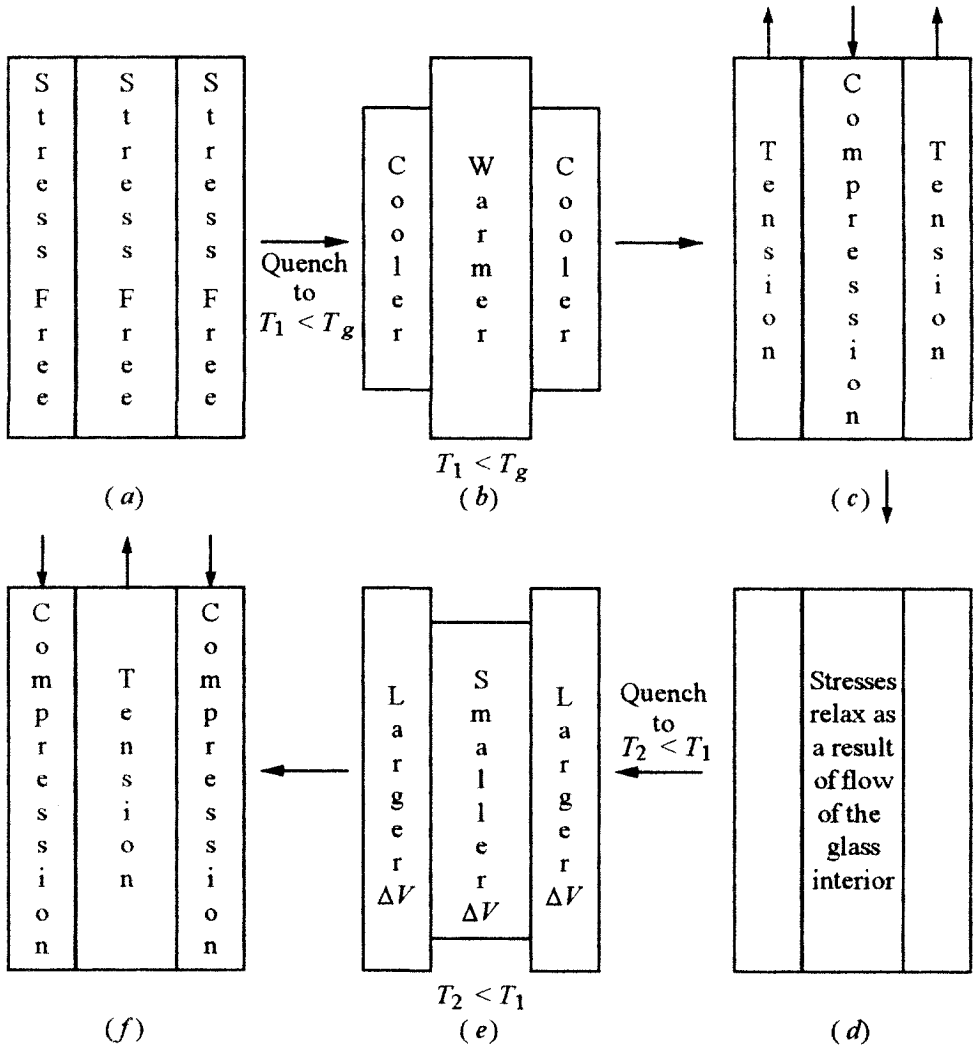

Figure 13.5 Thermal process that results in tempered glass. (*a*) Initial configuration. (*b*) The glass is quenched to a temperature that is below T_g, which results in the rapid contraction of the exterior. (*c*) Resulting transient state of stress. (*d*) The relaxation of these stresses occurs by the flow and deformation of the interior. (*e*) Second quenching step results in a more rapid cooling rate for the exterior than for the interior. This results in a glass with a smaller specific volume in the center than on the outside. (*f*) Final state of stress at room temperature.

By using this technique, the mean strength of soda-lime silicate glass can be raised to the range of 150 MPa, which is sufficient to permit its use in large doors and windows as well as safety lenses. Tempered glass is also used for the side and rear windows of automobiles. In addition to being stronger, tempered glass is preferred to untempered glass for another reason: the release of large amounts of stored elastic energy upon fracture tends to shatter the glass into a great many fragments which are less dangerous than larger shards. Windshields, however, are made of two sheets of tempered glass in between which a polymer layer in embedded. The function of the latter is to hold the fragments of glass together in case of fracture and to prevent them from becoming lethal projectiles.

13.6 Thermal Conductivity

The conduction of heat through solids occurs as a result of temperature gradients. In analogy to Fick's first law, the relationship between the heat flux and temperature gradients $\partial T/\partial x$ is given by

$$\frac{\partial Q}{\partial t} = k_{th} A \frac{\partial T}{\partial x} \tag{13.24}$$

where $\partial Q/\partial t$ is the heat transferred per unit time across a plane of area A normal to the flow of the thermal energy; and k_{th} is a material property (analogous to diffusivity) that describes the ability of a material to transport heat. Its units are J/(s·m·K) or equivalently W/(m·K). Approximate values for k_{th} for a number of ceramics are listed in Table 13.3.

Thermal conduction mechanisms

Describing the mechanisms of conduction in solids is not easy. Here only a brief qualitative sketch of some of the physical phenomena is given. In general, thermal energy in solids is transported by lattice vibrations, i.e. phonons, free electrons, and radiation. Given that the concentration of free electrons in ceramics is low and that most ceramics are not transparent, phonon mechanisms dominate and are the only ones discussed below.

Imagine a small region of a solid being heated. Atoms in that region will have large amplitudes of vibration and will vibrate violently around their average positions. Given that these atoms are bonded to other atoms, it follows that their motion must also set their neighbors into oscillation. As a result the disturbance, caused by the application of heat, propagates outward in a wavelike manner.[243] These waves, in complete analogy to electromagnetic waves, can be scattered by imperfections, grain boundaries,

Table 13.3 Approximate values for thermal conductivities of selected ceramic materials

Material	k_{th} W/(m·K)	Material	k_{th} W/(m·K)
Al_2O_3	30.0–35.0	Spinel ($MgAl_2O_4$)	12.0
AlN	200.0–280.0	Soda-lime silicate glass	1.7
BeO	63.0–216.0	TiB_2	40.0
MgO	37.0	Ti_3SiC_2	43.0
PSZ	2.0		
SiC	84.0–93.0	Cordierite (Mg-aluminosilicate)	4.0
SiAlON	21.0	Glasses	0.6–1.5
SiO_2	1.4	Forsterite	3.0
Si_3N_4	25.0		

[243] A situation not unlike the propagation of light or sound through a solid.

and pores or even reflected at other internal surfaces. In other words, every so often the disturbance will have the direction of its propagation altered. The average distance that the disturbance travels before being scattered is analogous to the average distance traveled by a gas molecule and is referred to as the *mean free path* λ_{th}.

By assuming the number of these thermal energy carriers to be N_{th}, and their average velocity v_{th}, it is reasonable to assume that, in analogy to the electrical conductivity equation of $\sigma = n\mu q$, k_{th} is given by

$$k_{th} = (\text{const})(N_{th}\lambda_{th}v_{th})$$

In general, open, highly ordered structures made of atoms or ions of similar size and mass tend to minimize phonon scattering and result in increased values of k_{th}. An excellent example is diamond, which has one of the highest thermal conductivity values of any known material. Other good examples are SiC, BeO, and AlN. More complex structures, such as spinels, and ones where there is a large difference in mass between ions, such as UO_2 and ZrO_2, tend to have lower values of k_{th}. Similar arguments suggest that the thermal conductivity of a solid will be decreased by the addition of a second component in solid solution. This effect is well known, as shown, e.g., by the addition of NiO to MgO or Cr_2O_3 to Al_2O_3.

Furthermore, the lack of long-range order in amorphous ceramics results in more phonon scattering than in crystalline solids and consequently leads to lower values of k_{th}.

Finally, it is important to mention the effect of porosity. Since the thermal conductivity of air is negligible compared to the solid phases, the addition of large (>25 percent) volume fractions of pores can significantly reduce k_{th}. This approach is used in the fabrication of firebrick. As noted above, the addition of large-volume fractions of porosity has the added advantage of rendering the firebricks thermal-shock-tolerant. Note that heat transfer by radiation across the pores, which scales as T^3, has to be minimized. Hence for optimal thermal resistance, the pores should be small and the pore phase should be continuous.

Experimental Details: Measuring Thermal Conductivity

Several techniques are used to measure k_{th}. One method that has gained popularity recently is the laser flash technique. In principle the technique attempts to measure the time evolution of the temperature on one side of the sample as the other side is very rapidly heated by a laser pulse. As it passes through the solid, the signal will be altered in two ways: There will be a time lag between the time at which the solid was pulsed and the maximum in the response. This time lag is directly proportional to the thermal diffusivity, D_{th}, of the material. The second effect will be a reduction

in the temperature spike, which is directly related to the heat capacity, c_p, of the solid. The heat capacity, thermal diffusivity, and thermal conductivity and density, σ, are related by:

$$k_{th} = \rho c_p D_{th}$$

Hence k_{th} can be calculated if the density of the solid is known and D_{th} and c_p are measured.

13.7 Summary

Temperature changes result in dimensional changes which result in thermal strains. Isotropic, unconstrained solids subjected to uniform temperatures can accommodate these strains without the generation of thermal stresses. The latter will develop, however, if one or more of the following situations are encountered:

- Constrained heating and cooling.
- Rapid heating or cooling. This situation can be considered a variation of that above. By rapidly changing the temperature of a solid, its surface will usually be constrained by the bulk and will develop stresses. The magnitude of these stresses depends on the severity of thermal shock or rate of temperature change. In general, the higher the temperature from which a ceramic is quenched the more likely it is to fail or thermal shock. Thermal shock can be avoided by slow heating or cooling. Solids with high thermal conductivities, fracture toughnesses and/or low thermal expansion coefficients are less prone to thermal shock.
- Heating or cooling of multiphase ceramics in which the various constituents have differing thermal expansion coefficients. The stresses generated in this case will depend on the mismatch in thermal expansion coefficients of the various phases. These stresses cannot be avoided by slow heating or cooling.
- Heating or cooling of ceramics for which the thermal expansion is anisotropic. The magnitude of the stresses will depend on the thermal expansion anisotropy, and can cause polycrystalline bodies to spontaneously microcrack. This damage cannot be avoided by slow cooling, but can be avoided if the grain size is kept small.
- Phase transformations in which there is a volume change upon transformation. In this case, the stresses will depend on the magnitude of the volume change. They can only be avoided by suppressing the transformation.

If properly introduced, thermal residual stresses can be beneficial, as in the case of tempered glass.

Finally, in the same way that solids conduct sound, they also conduct heat, i.e., by lattice vibrations. Heat conduction occurs by the excitation and interaction of neighboring atoms.

Problems

13.1. Give an example for each of (*a*) thermal strain but no stress, (*b*) thermal stress but no strain, and (*c*) a situation where both exist.

13.2. (*a*) Derive Eq. (13.6).

(*b*) A metallic rod ($\alpha = 14 \times 10^{-6}\,^{\circ}C^{-1}$, $Y = 50\,GPa$ at 800°C) is machined such that it perfectly fits inside an alumina tube. The assembly is then slowly heated; at 800°C the alumina tube cracks. Assume Poisson's ratio to be 0.25 for both materials.

(i) Describe the state of stress that develops in the system as it is heated.

(ii) Estimate the strength of the alumina tube.

Answer: 170 MPa

(iii) In order to increase the temperature at which this system can go, several strategies have been proposed (some of which are wrong): Use an alumina with a larger grain size; use another ceramic with a higher thermal expansion coefficient; use a ceramic that does not bond well with the metal; and use a metal with a higher stiffness at 800°C. Explain in some detail (using calculations when possible) which of these strategies you think would work and which would not. Why?

(iv) If the situation were reversed (i.e., the alumina rod were placed inside a metal tube), describe in detail the three-dimensional state of stress that would develop in that system upon heating.

(v) It has been suggested that one way to bond a ceramic rotor to a metal shaft is to use the assembly described in part (iv). If you were the engineer in charge, describe how you would do it. This is not a hypothetical problem but is used commercially and works quite well.

13.3. Consider a two-phase ceramic in which there are spherical inclusions *B*. If upon cooling, the inclusions go through a phase transformation that causes them to expand, which of the following states of stress would you expect, and why?

(*a*) Hydrostatic pressure in *B*; radial, compressive, and tangential tensile hoop stresses.

(*b*) Debonding of the interface and zero stresses everywhere.
(*c*) Hydrostatic pressure in *B*; radial, tensile, and tangential compressive hoop stresses.
(*d*) Hydrostatic pressure in *B*; radial, compressive, and tangential compressive hoop stresses.
(*e*) Hydrostatic pressure in *B*; radial, tensile, and tangential tensile hoop stresses.

13.4. (*a*) Plot the radial stress as a function of r for an inclusion in an infinite matrix, given that $\Delta\alpha = 5 \times 10^{-6}$, $\Delta T = 500^{\circ}C$, $Y_i = 300\,GPa$, $Y_m = 100\,GPa$, and $\nu_i = \nu_m = 0.25$.
(*b*) If the size of the inclusions were 10 μm, for what volume fraction would the "infinite" matrix solution be a good one? What do you think would happen if the volume fraction were higher? State all assumptions.

Answer: ≈5 to 10 vol.% depending on assumptions

13.5. (*a*) Is thermal shock more likely to occur as a result of rapid heating or rapid cooling? Explain.
(*b*) A ceramic component with Young's modulus of 300 GPa and a K_{Ic} of $4\,MPa \cdot m^{1/2}$ is to survive a water quench from 500°C. If the largest flaw in that material is on the order of 10 μm, what is the maximum value of α for this ceramic for it to survive the quench? State all assumptions.

Answer: $5 \times 10^{-6}\,^{\circ}C^{-1}$

13.6. (*a*) Derive Eq. (13.11).
(*b*) Which of the materials listed below would be best suited for an application in which a part experiences sudden and severe thermal fluctuations while in service?

Material	MOR, MPa	k_{th}, W/(m·K)	Modulus, GPa	K_{Ic}, MPa·m$^{1/2}$	α, K^{-1}
1	700	290	200	8	9×10^{-6}
2	1000	50	150	4	4×10^{-6}
3	750	100	150	4	3×10^{-6}

13.7. (*a*) Explain how a glaze with a different thermal expansion can influence the effective strength of a ceramic component. To increase the strength of a component, would you use a glaze with a higher or lower thermal expansion coefficient than the substrate? Explain.
(*b*) Fully dense, 1-cm-thick alumina plates are to be glazed with a porcelain glaze ($Y = 70\,GPa$, $\nu = 0.25$) of 1-mm thickness with

a thermal expansion coefficient of 4×10^{-6} °C. Assuming the "stress-freezing" temperature of the glaze to be 800°C, calculate the stress in the glaze at room temperature.

13.8. Using acoustic emission and thermal contraction data, Ohya *et al.*[244] measured the functional dependence of the microcracking temperature of aluminum titanate ceramics on grain size as the samples were cooled from 1500°C. The following results were obtained:

Grain size, μm	3	5	9
Microcracking temperature upon cooling, °C	500	720	900

(*a*) Qualitatively explain the trend observed.

(*b*) Are these data consistent with the model presented in Sec. 13.4.1? If so, calculate the value of the constant that appears in Eq. (13.22), given that $G_{c,\text{gb}} = 0.5\,\text{J/m}^2$, $Y = 250\,\text{GPa}$, and $\Delta\alpha_{\max} = 15 \times 10^{-6}$ °C.

Answer: $\approx 337\,(\text{°C})^{-2}$

(*c*) Based on these results, estimate the grain size needed to obtain a crack-free aluminum titanate body at room temperature. State all necessary assumptions.

Answer: $\approx 1.47\,\mu\text{m}$

13.9. Explain why volume changes as low as 0.5 percent can cause grain fractures during phase transformations of ceramics. State all assumptions.

13.10. (*a*) If a glass fiber is carefully etched to remove "all" Griffith flaws from its surface, estimate the maximum temperature from which it can be quenched in a bath of ice water without failure. State all assumptions. Information you may find useful: $Y = 70\,\text{GPa}$, $\nu = 0.25$, $\gamma = 0.3\,\text{J/m}^2$, and $\alpha = 10 \times 10^{-6}$ °C.

Answer: 5000°C

(*b*) Repeat part (*a*) assuming 1-μm flaws are present on the surface.

Answer: 82°C

(*c*) Repeat part (*b*) for Pyrex, a borosilicate glass for which $\alpha \approx 3 \times 10^{-6}$ °C. Based on your results, explain why Pyrex is routinely used in labware.

13.11. Qualitatively explain how the following parameters would affect the final value of the residual stresses in a tempered glass pane: (*a*) thickness of glass, (*b*) thermal conductivity of glass, (*c*) quench temperature, (*d*) quench rate.

[244] Y. Ohya, Z. Nakagawa, and K. Hamano, *J. Amer. Cer. Soc.*, **70**:C184–C186 (1987).

13.12. Rank the following three solids in terms of their thermal conductivity: MgO, $MgO \cdot Al_2O_3$, and window glass. Explain.

13.13. (*a*) Estimate the heat loss through a 0.5-cm-thick, 1000 cm^2 window if the inside temperature is 25°C and the outside temperature is 0°C. Information you may find useful: k_{th} conductivity of soda lime is 1.7 $W/(m \cdot K)$.

(*b*) Repeat part (*a*) for a porous firebrick that is used to line a furnace running at 1200°C. Typical values of k_{th} for firebricks are 1.3 $W/(m \cdot K)$. State all assumptions.

Additional Reading

1. W. D. Kingery, H. K. Bowen, and D. R. Uhlmann, *Introduction to Ceramics*, 2d ed., Wiley, New York, 1976.
2. C. Kittel, *Introduction to Solid State Physics*, 6th ed., Wiley, New York, 1986.
3. W. D. Kingery, "Thermal Conductivity of Ceramic Dielectrics," *Progress in Ceramic Science*, vol. 2, J. E. Burke, ed., Pergamon Press, New York, 1961.
4. D. P. H. Hasselman and R. A. Heller, eds., *Thermal Stresses in Severe Environments*, Plenum, New York, 1980.
5. H. W. Chandler, "Thermal Stresses in Ceramics," *Trans. J. Brit. Cer. Soc.*, **80**:191 (1981).
6. Y. S. Touloukian, R. W. Powell, C. Y. Ho, and P. G. Klemens, eds., *Thermophysical Properties of Matter*, vol. 2, *Thermal Conductivity — Nonmetallic Solids*, IFI/Plenum Press, New York, 1970.
7. D. W. Richerson, *Modern Ceramic Engineering*, 2d ed., Marcel Dekker, New York, 1992.